



The production and fate of molecular anions formed by electron attachment to low electron affinity compounds

by Michael Jeffrey Salyards

A dissertation submitted in partial fulfillment of the requirements for the degree of Doctor of Philosophy in Chemistry  
Montana State University

© Copyright by Michael Jeffrey Salyards (2003)

Abstract:

Resonance electron capture and thermal electron detachment rate constants have been determined for several low electron affinity (EA) compounds, including anthracene, benzophenone, quinoxaline. These measurements were taken by comparing the molecule of interest with SF<sub>6</sub> using pulsed high pressure mass spectrometry (PHPMS) to evaluate the time profiles for the relevant anions. These measurements were affected by re-capture of detached electrons as well as loss of these electrons by diffusion to the walls of the ion source. This dissertation also explains why these low EA molecules are not seen at atmospheric conditions. Using the PHPMS, the reactions of the molecular anions of anthracene, quinazoline, benzophenone, quinoxaline and azulene with oxygen and water have been studied. In the simultaneous presence of oxygen and water, these molecular anions, M, are rapidly destroyed and the ion, (O<sub>2</sub> H<sub>2</sub>O), is rapidly formed. The high rate with which this transition occurs cannot be explained by the simplest model envisioned that is based on well-known ion molecule reactions. These results can be explained, however, by inclusion into the model of a previously uncharacterized reaction between the molecular ion-oxygen complex, (M O<sub>2</sub>)<sup>-</sup>, and water. The results reported here explain why the molecular anions of compounds that have lower EA's than that of azulene are not readily observed in electron capture ion sources of one atmosphere buffer gas pressure. In addition, it is shown that the reactions characterized here lead to a state of chemical equilibrium between the M and (O<sub>2</sub> H<sub>2</sub>O) ions within the PHPMS ion source from which the EA values of the low-EA compounds can be determined. By this method the electron affinities of anthracene, quinazoline, benzophenone and quinoxaline are found to be 0.54, 0.56, 0.61 and 0.68 eV, respectively.

THE PRODUCTION AND FATE OF MOLECULAR ANIONS FORMED BY  
ELECTRON ATTACHMENT TO LOW ELECTRON AFFINITY COMPOUNDS

by

Michael Jeffrey Salyards

A dissertation submitted in partial fulfillment  
of the requirements for the degree

of

Doctor of Philosophy

in

Chemistry

MONTANA STATE UNIVERSITY  
Bozeman, Montana

June 2003

D378  
Sa397

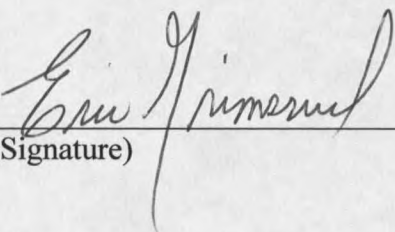
## APPROVAL

of a dissertation submitted by

Michael Jeffrey Salyards

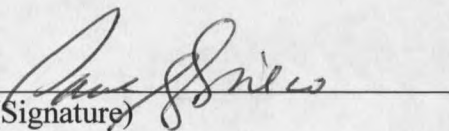
This dissertation has been read by each member of the dissertation committee and has been found to be satisfactory regarding content, English usage, format, citations, bibliographic style, and consistency, and is ready for submission to the College of Graduate Studies.

Dr Eric P. Grimsrud

  
(Signature)6/23/03  
Date

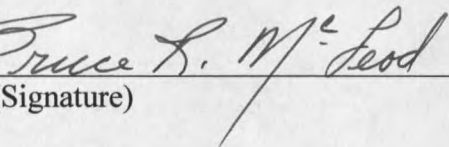
Approved for the Department of Chemistry and Biochemistry

Dr Paul A. Grieco

  
(Signature)6-11-03  
Date

Approved for the College of Graduate Studies

Dr Bruce R. McLeod

  
(Signature)6-30-03  
Date

## STATEMENT OF PERMISSION TO USE

In presenting this dissertation in partial fulfillment of the requirements for a doctoral degree at Montana State University, I agree that the library shall make it available to borrowers under rules of the Library. I further agree that copying of this paper is allowable only for scholarly purposes, consistent with the "fair use" as prescribed in the US Copyright Law. Request for the extensive copying or reproduction of this dissertation should be referred to Bell & Howell Information and Learning, 300 North Zeeb Road, Ann Arbor, Michigan 48106, to whom I granted "the exclusive right to reproduce and distribute my dissertation in and from microform along with the non-exclusive right to reproduce and distribute my abstract in any format in the whole or in part."

Signature Michael J. Salzarke  
Date 24 JUNE 2003

## ACKNOWLEDGEMENT

It is with a heart of thanksgiving that I finish my time at Montana State University. I cannot imagine how I would have finished or even started this research without the tireless efforts of my mentors, Dr Eric Grimsrud and Dr Berk Knighton.

In the immortal words of John Steinbeck's Seer in Canary Row, "I wouldn't think of doing something quite so big without having someone who's pretty handy with a sponge in my corner." My corner is filled with people who love and support me. Debbie, Amy and Mary – you are the stars in my sky, flooding my life with love, joy, and support. I am so proud of all you. Mom and Don, Dad and Renee, Rob and Mimi – you are my heritage. Any success that I have can be traced directly back to each of you. Your encouragement, love, support, and sacrifice are engraved on my heart. Jason and Jon – there is no way to go wrong with brothers like the two of you. Vern and Tanja Brekke, and all my ukes at Ternion – you have been good friends and dedicated sensies. I will never forget our journey from white to black. Pastor John Marks and my brothers and sisters at Abundant Life Fellowship – thanks for your prayers, friendship, and wise counsel. Finally, the United States Air Force Academy – I can't think of a more dedicated and professional group of people to work with. Thank you for letting me be on your team.

## TABLE OF CONTENTS

1. INTRODUCTION AND LITERATURE REVIEW .....	1
Pulsed High Pressure Mass Spectrometry .....	2
Hardware .....	3
Types of Data Collected .....	6
Plasma Conditions in the Ion Source.....	9
Electron Capture Cross Section, Feshbach States, and $M^{*-}$ Lifetimes .....	13
Interactions of Anions with a Buffer Gas .....	24
Stabilizing Collisions and the High Pressure Limit.....	24
Excitation and Thermal Electron Detachment.....	29
Methods for Measuring Resonance Electron Capture Rates .....	34
The Suitability of $SF_6$ as a Surrogate.....	36
Conclusion .....	37
2. RESONANCE ELECTRON CAPTURE AND THERMAL DETACHMENT.....	38
Benzophenone .....	38
Experimental.....	39
Results and Discussion .....	39
Apparent Loss of $BP^-$ to $SF_6$ .....	41
Time Profile Data and Differential Equations Model .....	43
Failure of Model at Low Number Densities .....	48
The New Model with Electron Diffusion .....	51
Predictions of Thermal Detachment .....	53
Efforts to Stabilize $BP^-$ with $SiF_4$ .....	54
Quinoxaline .....	55
Experimental.....	55
Results and Discussion .....	57
Anthracene.....	60
Experimental.....	61
Results and Discussion .....	62
Quinazoline.....	66
Experimental.....	67
Results and Discussion .....	68
Conclusion .....	72

## TABLE OF CONTENTS – CONTINUED

3. FAILURE TO DETECT THESE ANIONS AT ATMOSPHERIC CONDITIONS .....	74
Introduction .....	74
Experimental.....	78
Results and Discussion .....	79
Determination of Mechanism .....	81
Determination of Electron Affinities .....	94
Conclusions .....	98
REFERENCES CITED .....	99
APPENDICIES.....	111
APPENDIX A: HIGH PRESSURE LIMIT EQUATIONS.....	112
APPENDIX B: REVIEW OF PSUEDO 1 <sup>ST</sup> ORDER KINETICS.....	116
APPENDIX C: MODELING WITH DIFFERENTIAL EQUATIONS.....	118

## LIST OF TABLES

Table	Page
1-1. Review of Feshbach resonance descriptions in the literature .....	20
1-2. Thermodynamic and kinetic properties of a typical molecule .....	33
2-1. Parameters used for the IBM Kinetic Simulator .....	45
2-2. Thermodynamic and kinetic properties of benzophenone .....	54
2-3. Thermodynamic and kinetic properties of quinoxaline.....	59
2-4. Thermodynamic and kinetic properties of anthracene .....	66
2-5. Summary of kinetic and thermodynamic properties for each molecule.....	72



## LIST OF FIGURES

Figure	Page
1-1. Schematic of the PHPMS .....	3
1-2. Photograph of the PHPMS front flange .....	4
1-3. Standard and logarithmic time profiles of the SF <sub>6</sub> anion .....	6
1-4. Logarithmic and normalized time profiles of two anions .....	8
1-5. Normalized time profiles showing equilibrium of several ions .....	9
1-6. Nitric oxide data showing the ion dominated plasma transition .....	12
1-7. Fluorocarbon ion lifetimes versus vibrational degrees of freedom.....	22
1-8. Unimolecular rate constant versus pressure for a theoretical case.....	26
1-9. Comparison of thermal electron detachment predictions.....	33
2-1. Structure of benzophenone.....	38
2-2. Mass spectra of benzophenone and SF <sub>6</sub> at different temperatures.....	40
2-3. Time profiles of the ions in Figure 2-2 .....	41
2-4. Measured $k_{\text{transfer}}$ values for electron transfer to SF <sub>6</sub> .....	43
2-5. Time profiles of BP <sup>-</sup> and SF <sub>6</sub> <sup>-</sup> at different temperatures .....	44
2-6. Extrapolation of initial concentrations for logarithmic time profiles.....	47
2-7. Measured electron capture rate constants for benzophenone.....	47
2-8. The linear model of $k_{\text{cc}}$ and $k_{\text{det}}$ for benzophenone .....	50
2-9. Histogram of calculated electron diffusion rate constants .....	52
2-10. Predicted versus measured BP <sup>-</sup> slopes from logarithmic time profiles.....	53
2-11. Prediction of thermal electron detachment rate constants for benzophenone.....	54

## LIST OF FIGURES continued

2-12. Mass spectra of $(BP \bullet SiF_4)^-$ and $SF_6^-$ .....	56
2-13. Structure of quinoxaline .....	57
2-14. Measured electron capture rate constants for quinoxaline .....	58
2-15. Predicted versus measured $Qx^-$ slopes from logarithmic time profiles .....	59
2-16. Prediction of thermal electron detachment rate constants for quinoxaline .....	60
2-17. Structure of anthracene .....	61
2-18. Effects of 179? amu impurity on anthracene .....	62
2-19. Measured electron capture rate constants for anthracene .....	63
2-20. Measured electron capture rate constants for anthracene .....	64
2-21. Predicted versus measured $A^-$ slopes from logarithmic time profiles .....	65
2-22. Prediction of thermal electron detachment rate constants for anthracene .....	67
2-23. Structure of quinazoline .....	67
2-24. Mass spectrum of $Qz^-$ quinazoline and $O_2$ cluster .....	69
2-25. Measured electron capture rate constants for quinazoline .....	70
2-26. Loss of $Qz^-$ to thermal detachment .....	71
3-1. IMS spectra of anthracene and benzophenone .....	77
3-2. Negative ion mass spectra of oxygen and water and anthracene .....	80
3-3. Time profile of the family of anthracene, oxygen and water anions .....	82
3-4. Computer generated time profiles of the Model A mechanism .....	85
3-5. Computer generated time profiles of the Model B mechanism .....	87
3-6. Time profile of the family of quinazoline, oxygen and water anions .....	88

## LIST OF FIGURES continued

3-7. Time profile of the family of benzophenone, oxygen and water anions.....	90
3-8. Time profile of the family of quinoxaline, oxygen and water anions .....	91
3-9. Time profile of the family of azulene, oxygen and water anions.....	93
3-10. Electron affinity determinations for each molecule in this study.....	96

## ABSTRACT

Resonance electron capture and thermal electron detachment rate constants have been determined for several low electron affinity (EA) compounds, including anthracene, benzophenone, quinoxaline. These measurements were taken by comparing the molecule of interest with SF<sub>6</sub> using pulsed high pressure mass spectrometry (PHPMS) to evaluate the time profiles for the relevant anions. These measurements were affected by re-capture of detached electrons as well as loss of these electrons by diffusion to the walls of the ion source. This dissertation also explains why these low EA molecules are not seen at atmospheric conditions. Using the PHPMS, the reactions of the molecular anions of anthracene, quinazoline, benzophenone, quinoxaline and azulene with oxygen and water have been studied. In the simultaneous presence of oxygen and water, these molecular anions, M<sup>-</sup>, are rapidly destroyed and the ion, (O<sub>2</sub> • H<sub>2</sub>O)<sup>-</sup>, is rapidly formed. The high rate with which this transition occurs cannot be explained by the simplest model envisioned that is based on well-known ion molecule reactions. These results can be explained, however, by inclusion into the model of a previously uncharacterized reaction between the molecular ion-oxygen complex, (M•O<sub>2</sub>)<sup>-</sup>, and water. The results reported here explain why the molecular anions of compounds that have lower EA's than that of azulene are not readily observed in electron capture ion sources of one atmosphere buffer gas pressure. In addition, it is shown that the reactions characterized here lead to a state of chemical equilibrium between the M<sup>-</sup> and (O<sub>2</sub> • H<sub>2</sub>O)<sup>-</sup> ions within the PHPMS ion source from which the EA values of the low-EA compounds can be determined. By this method the electron affinities of anthracene, quinazoline, benzophenone and quinoxaline are found to be 0.54, 0.56, 0.61 and 0.68 eV, respectively.

## INTRODUCTION AND LITERATURE REVIEW

One of the most fundamental processes in chemistry, especially analytical chemistry, is the capture of an electron by a neutral molecule to form the parent anion. This process, often referred to as resonance electron capture (REC), can be naively written as Reaction 1-1:



where  $k_{\text{ec}}$  is the electron capture rate constant, and  $k_{\text{det}}$  is the thermal electron detachment rate constant. Some of the sections that follow will show that this reaction also involves an intermediate. The importance of electron capture and negative ion formation to analytical chemistry has its roots in the 1948 discovery of a young English scientist. At that time, James Lovelock was commissioned by the British Medical Research Council to study the common cold. Specifically, he was asked to investigate the popularly held notion that colds are caught by being exposed to a cold draft. Lovelock's efforts, which included using radioactive  $\alpha$  particle emitting paint from WWII aircraft gauges, to measure changes in the density of air led to the invention of an ionization apparatus. He did not learn anything useful about the common cold, but he did succeed in making a device that was especially sensitive to halocarbon gases [1]. Eventually the ionization source was changed to a  $\beta$  emitter, and the electron capture detector (ECD) was born. ECD use in the next 10 years moved to biochemistry and then to the detection of environmentally dangerous molecules [2].

In 1962, Rachel Carson published *Silent Spring* [3]. Writing somewhat poetically about the environment, she described an impending chemical apocalypse. The ECD had proven so sensitive that researchers reported finding trace levels of pesticides in samples ranging from penguin fat to mother's milk. Carson's work thrust the ECD into the scientific limelight, and the study of electron capture and the formation of gaseous ions became popular. Presently, the study of electron capture is important in a wide range of disciplines including gaseous dielectrics [4], excimer lasers [5], discharges used for etching [6], and atmospheric chemistry [7].

The sections that follow will provide a discussion and review of: a) the pulsed high pressure mass spectrometer (PHPMS) which was used to collect data for all of the experiments in this dissertation, and b) relevant theories and literature surrounding the phenomenon of electron capture and its opposite, thermal electron detachment. Chapter 2 describes experiments that were designed to measure resonance electron capture and thermal electron detachment rate constants for several low electron affinity (EA) molecules. Finally, Chapter 3 presents a series of experiments that explain why these low EA molecules are difficult to detect at atmospheric conditions.

### Pulsed High Pressure Mass Spectrometry

Kebarle developed the PHPMS during the late 1960's, and its construction and operation have been fully described previously [8]. This section is not intended to repeat the details of construction provided in this reference. However, brief descriptions of the

physical apparatus, the ionization source, the electron optics, and the types of data that can be collected, may be helpful for understanding the experiments in Chapters 2 and 3.

### Hardware

Figure 1-1 is a schematic of the PHPMS. The gas handling plant is a 6.5 liter glass bulb. It is typically pressurized to approximately 800 torr with a buffer gas.

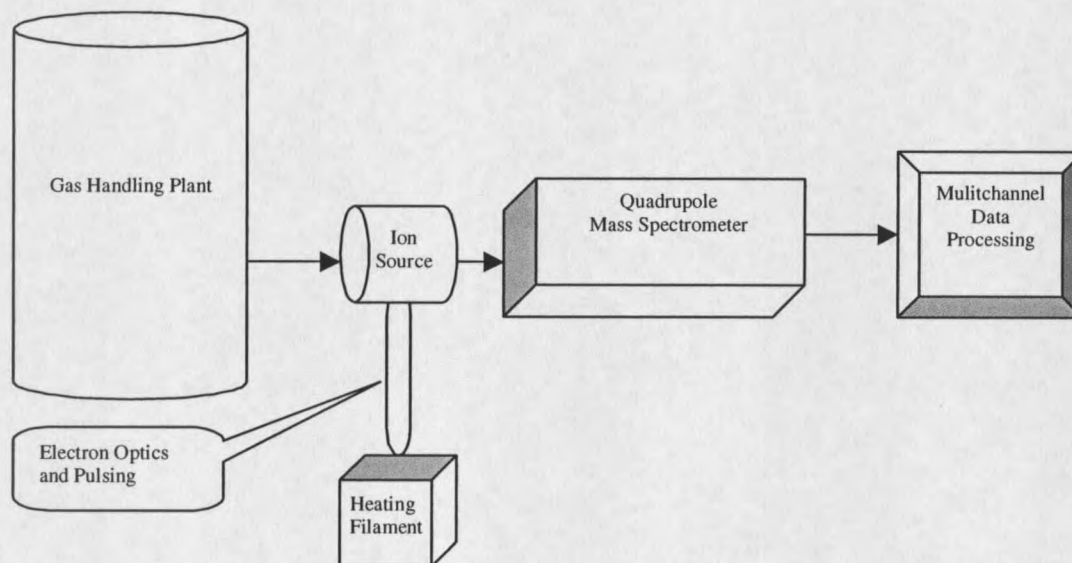


Figure 1-1. A schematic representation of the PHPMS hardware and main components.

For all of the experiments in this dissertation, methane was used as the buffer gas. Other gases including helium, nitrogen, oxygen, and argon with 15% methane have been used in previous experiments [9]. The gas handling plant is fitted with an injection port that allows introduction of both gas and liquid samples. Solid samples are dissolved in a suitable solvent (toluene was often used for the experiments in this dissertation) and the solution is injected. The gas handling plant is typically heated to about 120°C to ensure

complete volatilization of sample molecules that often have relatively low vapor pressures.

Once the gas handling plant is loaded with the desired analytes, a valve is opened, and the mixture flows through a heated transfer line into the ion source as shown in Figure 1-2.

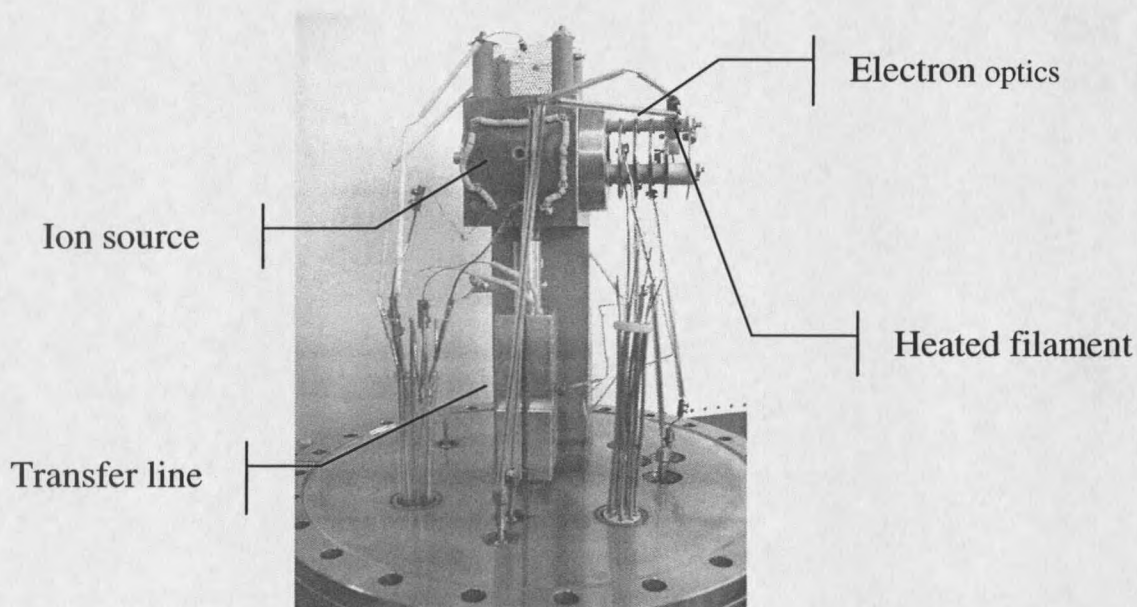


Figure 1-2. A photograph of the front flange of the PHPMS revealing the transfer line, ion source and the electron filament and pulsing optics. In this orientation, the gas mixture would flow from the bottom of the picture frame to the top. The electron optics are  $90^\circ$  off axis to the right at the top of the picture. For reference, the flange circumference is 10 inches.

The pressure in the ion source is controlled by the amount of gas flowing out of the gas handling plant. Typical ion source pressures are between 1-5 torr, and the ion source is heated between  $30-150^\circ\text{C}$ . Both of these parameters are adjusted as dictated by a given experiment.



Electrons are produced from a heated filament that is  $-2.95$  kV relative to the ion source. A gate lens is approximately  $0.75$  cm in front of the filament. The gate lens is held at  $-3.0$  kV. Approximately every  $75$ - $100$  msec the gate lens potential is pulsed to  $-2.90$  kV for about  $20$   $\mu$ sec. This voltage change sends a pulse of  $2.95$  keV high energy electrons through a stack of focusing lenses into the ion source via a small entrance aperture. Because the number density of the buffer gas is about  $7$ - $9$  orders of magnitude greater than the number density of the sample molecules, these high energy electrons are believed to interact primarily with the buffer gas. The chemical cascade that follows was first described by Munson and Field in their seminal paper on chemical ionization [10]. Basically, a whole host of positive methane and ethane related ions are formed as well as a complementary population of thermal electrons. In methane buffer gas, each high energy electron produces about  $85$  thermal electrons. If the sample molecules have a positive EA, they will capture some of these thermal electrons and form anions. Depending on their proton affinity, sample molecules may also form cations by interacting with the positively charged buffer gas related ions. As will be detailed in the next section, these newly formed ions diffuse to the wall of the ion source. A representative population of these ions passes through an exit slit into a quadrupole mass spectrometer. By narrowing the exit slit, the ion source can be operated in the  $10$ - $20$  Torr region. However, the narrow slit decreases the ion signal. Ions are detected using an electron multiplier and an ion counting channeltron.

### Types of Data Collected

The electron pulsing and related detection hardware and software are what make the PHPMS unique. Multichannel scalar software allows discrete channels of data to be collected after the electron pulse event. The time length of the channels can be varied from 5  $\mu\text{sec}$  to several hundred msec. By selecting long channel times ( $\approx 160$  msec) and scanning the quadrupole, typical mass spectra are obtained. However if much shorter channel times ( $\approx 100$   $\mu\text{sec}$ ) are used and the appropriate  $m/z$  is selected on the quadrupole, the population of a given ion in the source can be tracked in time as it is formed and diffuses to the wall. As might be expected, the diffusion of ions to the wall is a first order loss process and indicated in Figure 1-3.

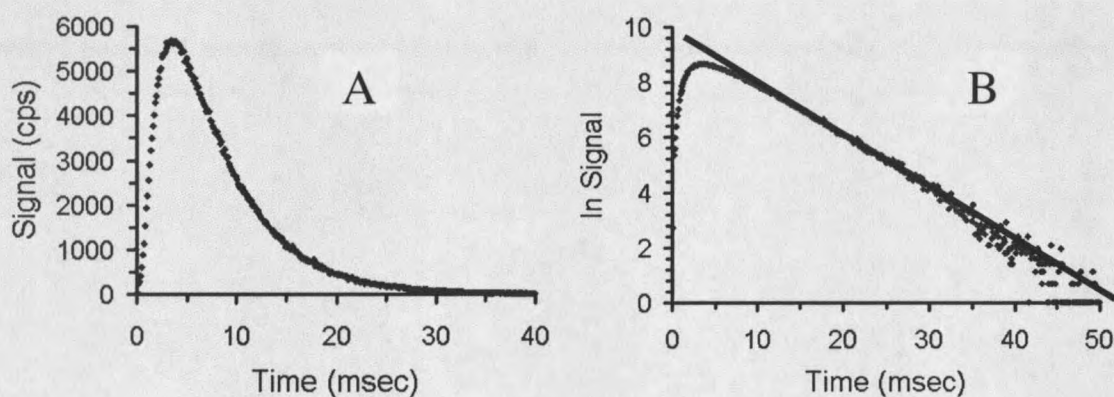


Figure 1-3. Standard time profile of SF<sub>6</sub> anion. The ion source pressure is  $\approx 3.0$  Torr. The ion source temperature is 60°C. (A) is the standard plot of signal versus time. (B) is the same data plotted as the ln of the signal versus time. A line has been superimposed on the data to highlight the linear relationship.

The diffusion rate constant,  $k_{diff}$ , is approximately  $150 \text{ sec}^{-1}$  at 3 torr and  $60^\circ\text{C}$ . Diffusion of ions depends primarily on three variables, the temperature squared, the inverse of pressure, and the reduced mobility of the ion. Equation 1-2 can be derived from equations provided by McDaniel and Munson [11].

$$k_{diff} \propto \frac{T^2}{P} K_0 \quad (1-2)$$

In this equation, the reduced mobility term,  $K_0$ , contains information about the reduced mass of the ion of interest as well as a term that describes how strongly the ion interacts with the buffer gas [12]. For all the experiments in this dissertation, ions were considered to have the same mobility to a first approximation. Therefore, diffusion is treated as a function of inverse pressure and temperature squared.

In addition to diffusion, ions can be lost if they react with a neutral molecule or another ion. Further, the diffusional loss of other ions may be partially offset if they are being produced by a chemical reaction. Sometimes it is helpful to compare the time profiles of two ions as in Figure 1-4. Close examination of the logarithmic plot in Figure 1-4 (A) reveals that the population of the ion represented by the circles is disappearing faster than the population of the ion represented by the squares. Because these ions are both being lost to diffusion, sometimes these other loss and production terms are subtle and difficult to see on a logarithmic plot. The normalized plot in Figure 1-4 (B) is prepared by dividing a given ion signal by the total ion signal. The inference from Figure 1-4 (B) is that the circle ions are reacting away and the square ions are being produced.

































































































































































































































































